Ind. J. Pharm. Edu. Res., 2026; 60(2):642-651.
https://www.ijper.org

Original Article

Green Synthesized Zinc Oxide Nanoparticles Using *Musa acuminata* Corm Extract and Its Anti-Cancer Activity

Hassani Rym[1,2,*]

[1]Environment and Nature Research Centre, Jazan University, Jazan, SAUDI ARABIA.
[2]Nanotechnology Research Unit, Jazan University, Jazan, SAUDI ARABIA.

ABSTRACT

Background Information: Osteosarcoma is the most common type of bone cancer, typically affecting children and young adults. It primarily develops in the long bones of the arms and legs. The banana (Musa spp) is widely popular in tropical regions around the world. One of its species, the Cavendish banana (*Musa acuminata*), is a wild plant that thrives in tropical and subtropical climates. In recent years, the health benefits of *M. acuminata* have gained considerable attention. Different parts of the plant have been used in traditional medicine to treat various ailments. While some parts of *M. acuminata* have demonstrated anti-cancer properties, the corm has not been extensively studied. **Objectives:** This study investigates the anti-cancer effects of biosynthesized *Musa acuminata* corm extract-coated zinc oxide nanoparticles on the Saos2 osteosarcoma cell line. **Materials and Methods:** Zinc oxide nanoparticles coated with *Musa acuminata* corm extract were described in the present study using SEM, FTIR, DLS, and UV-vis to assess their characteristics. The cytotoxicity and cell proliferation of ZnO NPs and chemically synthesised ZnONPs at different doses were verified using MTT and trypan blue. Phase contrast microscopy and DAPI staining were used to examine the morphological assessment of Saos2 cells and apoptosis, respectively. Using rhodamine 123 staining and fluorescence microscopy, the membrane integrity of mitochondria was examined. Lipid peroxidation, glutathione, and nitric oxide levels were used to assess ZnO NPs' antioxidant capacity. **Results:** Nanoparticles characterization reveals the synthesis of *Musa acuminata* corm extract coated zinc oxide nanoparticles and moreover XRD patterns reveals the hexagonal shape with an average size of 75.50 and 46.42 nm respectively. The MTT assay showed significant suppression of Saos2 cells, with an IC_{50} of 300 µg/mL indicating 49.36% inhibition. The trypan blue exclusion assay exhibited a progressive decline in the percentage of viable cells, and phase contrast microscopy revealed morphological distortions in the treated cells. The presence of apoptotic cells was observed in DAPI staining and ROS staining. Oxidative stress biomarkers including NO and LPO were significantly increased whereas, antioxidant biomarker such as GSH decreased in the treated groups. **Conclusion:** Based on the research outlined above, the anticancer properties of ZnO NPs coated with *Musa acuminata* corm extract effectively targeted osteosarcoma cells.

Keywords: *Musa acuminata*, Reactive oxygen species, Wound healing, Osteosarcoma, Zinc oxide nanoparticle.

Correspondence:
Dr. Hassani Rym
[1]Environment and Nature Research Centre, Jazan University, P.O. Box. 114, Jazan 45142, SAUDI ARABIA.
[2]Nanotechnology Research Unit, Jazan University, P.O. Box. 114, Jazan, SAUDI ARABIA.
Email: rhassani@jazanu.edu.sa
ORCID: 0000-0002-9340-8835

Received: 24-06-2025;
Revised: 04-08-2025;
Accepted: 17-09-2025.

INTRODUCTION

Osteosarcoma is the most prevalent type of bone cancer. This type of cancer primarily affects children and young adults, typically developing in the long bones of the arms and legs. It represents the eighth most prevalent childhood cancer among all types of pediatric malignancies. Osteosarcoma in men is 1.4 times more common than in women and commonly treated with high-dose regimens of methotrexate, cisplatin, and doxorubicin.[1,2] Chemotherapy, Radiotherapy and surgery is also used to treat the osteosarcoma. Medication such as vincristine, doxorubicin, and cyclophosphamide are used in substitutes for etoposide and ifosfamide.[3] Nevertheless, the risks of above treatments cause infection, nausea, vomiting, hair loss, appetite loss, renal damage, myelosuppression, peripheral neuropathy, and hypomagnesemia and these side effects have an impact on both the mental and physical health of osteosarcoma patients.[4] Globally, the number of cancer cases rising year is a difficulty despite advancements in cancer therapies such as surgery, radiation therapy, chemotherapy, and other forms of treatment. It follows that the present needs are for innovative anticancer medications that are highly effective, more targeted, less toxic, and easily accessible. Many studies have shown that eating a diet high in plant-based medicines such as phytochemicals and bioactive

DOI: 10.5530/ijper.20262292

compounds reduces the risk of cancer by causing apoptosis, slowing cell proliferation, and disrupting the cell cycle.[5,6]

The banana, particularly *Musa* spp., is a popular fruit in tropical regions worldwide.[7] *Musa acuminata*, commonly known as the Cavendish banana, is native to tropical and subtropical climates. Different parts of the plant have been used in traditional medicine to treat various health conditions.[8] Some components of *Musa acuminata* are known to possess antidiabetic, anti-inflammatory, antioxidant, and anticancer properties.[9] The corm, which is covered by thin leaves that loosely encase its vertical, expanded, and compact structure. The ethanolic extract was rich in tannins, sterols, flavonoids, terpenoids, glycosides, and quinones and shown potential antibacterial activity against eight clinically harmful isolates.[10]

The banana, especially *Musa* spp., is a common favorite in tropical areas of the world Tropical and subtropical regions are home to the wild plant species *Musa acuminata*, often known as the Cavendish banana. In recent years, *M. Acuminata* health benefits have garnered a lot of attention. The corm has not received much attention in medicinal field. Therefore, we choose to analyze the anticancer activity of corm. Although the compounds in medicinal plants have anticancer capabilities, they cannot directly target cancer cells. This might be resolved by targeted cell delivering using nanocarriers.

However, an increasing number of researchers are now focusing on plant-based nanomaterials and anticancer medications.[11,12] Metal-based nanoparticles are becoming more and more popular in therapeutic delivery due to their broad, targeted availability, improved biocompatibility, extensive surface functionalization, and controlled drug release.[13,14] Metal oxide nanoparticles, such as ZnO-NPs, are known for their excellent cytotoxicity and potential for various applications. They are less hazardous and economically viable, and are authorized by the FDA as GRAS (Generally Recognized as Safe) due to their enhanced biocompatible nature. ZnO-NPs can be used as therapeutic compounds, drug formulations, and diagnostic agents in bioimaging applications.[15] They are suitable for cancer detection, drug delivery, and treatment. ZnO-NPs can be fabricated using chemical, physical, and biological methods, but these methods have downsides like high pressure or temperature requirements, waste generation, and energy consumption. Biological methods offer an inexpensive and environmentally sustainable method for synthesizing nanoparticles, with plant extracts being a popular reducing agent in these methods.[15] Through a range of techniques, including characterization, cytotoxicity tests, morphometric analysis, ROS detection using the DCFH-DA method of fluorescent staining, and biochemical tests including LPO, NO, and GSH, this work seeks to understand the anti-proliferative effects of MACE-ZnO NPs. The findings indicate that ZnO NPs trigger apoptosis in Saos2 cell line and targeted drug delivery by Nps to cancer cells can reduce the adverse effects of chemotherapy.

MATERIALS AND METHODS

Musa acuminata corm extract preparation

The corm of *Musa acuminata* was carefully collected and cleaned to get rid of any dirt and adherent soil particles. The corm was sliced into tiny pieces and let too dry at 65°C for the whole night. The sample was dried and then pulverized into a powder. The extract was kept at room temperature and it was labeled MACE (*Musa acuminata* corm extract).

Synthesis of MACE-ZnO NPs

To synthesize ZnO NPs method was slightly modified by G. Yashini *et al.*, (2019),[16] 90 mL of 0.02 M zinc acetate dihydrate ($ZnC_4H_6O_4$) was added, and the mixture was agitated for 10 min at 200 rpm using a magnetic stirrer. Following the addition of 10 mL of the MACE extract, 2.0 M NaOH was used to bring the solution's pH down to 12 until a pale white aqueous solution was created. A white precipitate appeared after 3 hr of stirring. Centrifugation at 4,000 rpm for 25 min was used to separate the white precipitate. The precipitate was first washed for 1 min using 5 mL of distilled water and 95% ethanol to remove impurities. To produce pale white ZnO NPs powder, the precipitate was dried overnight at 100°C in a drying oven.

Characterization of MACE-ZnO NPs

Several parameters have been used to analyze the physiochemical characteristics of ZnO-NPs. The UV-vis spectrophotometer was used to confirm the optical characteristics of ZnO-NPs. The existence of functional chemicals was examined using an FT-IR spectrometer. The stability of ZnO-NPs was assessed by analyzing the particle size distribution. The LEO 1355 VP with energy-dispersive SEM was used to examine the surface characteristics. ZnO-NPs' crystallite quality was evaluated using an X-ray diffractometer.

Cell line

In the United States, the ATCC provided the osteosarcoma cell line Saos2. The cells were incubated at 37°C in humidified 5% CO_2 after being cultivated in 10% DMEM with 2% Pen/Strep antibiotic. Until the required confluency was reached, the fresh DMEM was changed every two to three days.

MTT Assay

Initially, the anti-cancer potential of Corm ZnO-NPs and chemically synthesised ZnONPs on Saos2 cells was confirmed using the MTT test.[17] Each well of a 96-well plate contained 1x105 cells. Following a confluency of 80-90%, the cells were exposed to different NPs doses during 24 hr, including 50, 100, 150, 200, 250, 300, 350, 400, 450, and 500 µg/mL. Each well received 15 µL of MTT solution, which was then incubated for 4 hr in the dark. After that, 200 µL of DMSO was added to dissolve the formazan

crystal. The percentage of inhibition was computed by reading the plate at 490 and 630 nm using a microtiter plate reader.

Inhibition (%) = (1- {(OD Treated)490 - (OD Treated)630/ (OD Control) 490-(OD Control)630} x 100)

Trypan blue exclusion assay

In order to confirm the cytotoxicity of ZnO-NPs, the trypan blue exclusion test was used to assess the viability of treated cells.[18] After reaching 80% confluency, Saos2 cells were exposed to 200, 250, and 300 µg/mL of corm ZnO-NPs for 24 hr. Following that, PBS wash was applied to both treated and untreated cells. Trypan blue dye (0.4%) was added after the cells had been trypsinized and resuspended in fresh DMEM. The viable and non-viable cells were manually counted using a hemocytometer. The viability % was computed.

The number of viable cells divided by the total number of cells x 100 is the viability percentage.

Morphometric Analysis

To confirm that corm ZnO-NPs had anti-cancer properties, the morphometric changes of treated cells were examined in further detail. For 24 hr, the cells were subjected to different concentrations of corm ZnO-NPs (200, 250, and 300 µg/mL). Following the removal of the preexisting DMEM, PBS washing was performed on both the treated and control cells. A phase contrast microscope (Olympus, Tokyo, Japan) was used for taking and examining pictures of the morphometric deformations in the treatment cells.[19]

Wound healing Scratch Assay

In 24-well plates, Saos2 cells (3×105 cells/well) were seeded and allowed to develop in a monolayer for 24 hr. Next, each well was scratched with a sterile 20-200 µL pipette tip held vertically. Following a 5-min shake at 500 rpm and a 500 µL PBS wash, the detached cells were removed. After adding 500 µL of new media, with diluted MACE-ZnONPs, the mixture was incubated for 48 hr. The plate was cleaned with 500 µL of preheated PBS and gently shook for 30 sec before to picture collection. After that, the fresh medium was put in once more, and photos were taken. Using an inverted microscope set to 4x magnification, the scratch closure was observed and photographed every 24 hr.[20]

Staining with DAPI

The apoptotic potential of ZnO-NPs towards Saos2 cells was examined using the DAPI staining technique.[21] In a 24-well plate, 1x105 cells were seeded, and they were subjected for 24 hr to 200, 250, and 300 µg/mL. The cells were then washed in cooled PBS and fixed for 10 min in refrigerated methanol. The cells were permeabilized with 4% formaldehyde, stained with 0.5 µg/mL DAPI dye, and then washed for additional examination. Eventually, a fluorescent microscope (Nikon, Japan) was used to capture the images.

ROS Assay by Staining method

The ROS found in cells were investigated using the DCFH-DA (dichloro-dihydro-fluorescein diacetate) assay. Six-well plates containing Saos2 cells (2 × 106 cells/well) were maintained at 37°C with 5% CO_2. After transferring the developed cells to 24-well plates, different doses of corm-Zn NPs were then added to each well. Nanoparticles were loaded with 25 µM DCFH-DA in DMEM for 30 min at 37°C after being exposed to Saos2 cells and then rinsed with PBS. After being washed with DMEM, the treated cells were exposed to spectrophotometry for 30 min at 37°C. Fluorescence was measured at 485 nm excitation and 535 nm emission every 5 min.[22]

Nitric oxide Assay

Nitric oxide levels in treated and untreated cells[23] were measured using the Griess reagents with a few minor modifications. 50 µL of ZnO-NPs treated with 200, 250, and 300 µg/mL and control cell culture supernatant were mixed with 50 µL of Griess A reagent (1% sulphanilamide in 5% H_3PO_4). For 5 min, the complex was left at ambient temperature in a dark setting. After adding 50 µL of Griess B reagent (0.1% NEDA in 5% H_3PO_4), the mixture was incubated under the same conditions as previously described. At 520 and 550 nm, the purple-colored complex was measured. The units used to express the concentrations are µM.

Lipid peroxidation Assay

Lipid peroxidation activity was estimated using the TBARS assay, which was performed with minor adjustments as specified in the procedure of.[24] We completely homogenized the corm ZnO-NPs-treated and control cells using cooled KCl buffer. After adding 0.2 mL of 8.1% SDS, 1.5 mL of 20% acetic acid, 1.5 mL of 0.8% TBARS, and 0.7 mL of sterile H_2O to 100 µL of final homogenate, the mixture was allowed to boil for 1 hr. The wavelength of the absorption was 532 nm. The units used to represent the concentrations are µM.

GSH

The procedure outlined in was used, with minor adjustments, to conduct the reduced glutathione test. Both the treated and control cells underwent centrifugation and trypsinization. As a consequence, 0.1 M potassium phosphate buffer (pH 7.4) was used to homogenize the pellets.[25] A 4% sulfosalicylic acid solution was added to 0.5 mL of homogenate, and the mixture was incubated for 1 hr at 4°C. After centrifuging the mixture, 0.03 mL of the supernatant was taken out, and 0.066 mL of DTNB and 0.9 mL of 0.1 M potassium phosphate buffer (pH 7.4) were added. The absorbance at 412 nm was measured. The symbol for the reduced glutathione was mM.

RESULTS

Characterization study of MACE-ZnO NPs

The UV spectroscopy measurements displayed in (Figure 1A) were used to demonstrate the production of the biosynthesized zinc oxide nanoparticles. In the UV spectrum, ZnO-NPs displayed high absorption bands at 265 nm, signifying the production of ZnONPs. Figure 1B depicts images obtained using scanning electron microscopy, which revealed the aggregated form of nanoparticles with irregular spherical and Hexagonal shaped particles indicating the presence of ZnO. To further understand the distribution of the primary components in the ZnO-MACE synthesis, energy dispersive X-ray spectroscopy was performed. Figure 1C indicated that there was 50.37% Zn and 49.63% O, indicating that the bonding between the zinc nanoparticles and the corm extract was consistent (Figures 2A and 2B). Fourier transform infrared spectroscopic analysis represented the spectrum of MACE alone and Figure 5 representing MACE mixed with ZnONPs. Figure 4 shows a peak at 1021.99, which denotes the stretching vibration of the C-O group, whereas in Figure 5, 3264.96 and 1591.11 peaks correspond to the -NH and -OH, H-O-H stretching vibrations, respectively, 1307.27 indicates the stretching vibration of C-H bonding, and 512.07 clearly indicates the synthesis of metal oxide nanoparticles. The peaks at 3264.96 confirmed the existence of MACE, which are active chemicals that cap with nanoparticles. The average zeta potential value found in this investigation was -0.0122 V, as seen in Figure 1E. The polydispersity index of the green-fabricated ZnO-NPs was 28.3%, and the particle size distribution was determined to be 0.4144 micrometers (Figure 1F). XRD analysis uses the following lattice planes and related angles: 31.70° (100), 34.43° (002), 36.23° (101), 47.66° (102), 57.66° (110), 62.93° (103), 66.56° (200), 68.02° (112), and 69.21° (201) (Figure 1D). The findings demonstrate that the ZnO has a spherical and hexagonal shaped crystal structure.

Cytotoxicity analysis

The MTT reagent was used to investigate the cytotoxic effects of ZnO-NPs mediated by MACE on Saos2 cells. The high-dose of 500 µg/mL showed 90.07% inhibition. At 250 µg/mL, the IC_{50} indicated 49.11% inhibition, while at 200 µg/mL, it showed 12.12% (Figure 3A). The doses of 5, 10, 15, 20, and 25 µg/mL, on the other hand, showed viability in a higher proportion. chemically synthesised nanoparticles 50 µg/mL concentration showed 42.32% inhibition and 80 to 90 µg/mL showed an IC_{50} value of chemically synthesised nanoparticles Figure 3B.

Viability assay

In the viability experiment, dosages of 200, 250, and 300 µg/mL were chosen based on the MTT results (Figure 3C). At 300 µg/mL, the viability was 18.17%, while at 200 and 250 µg/mL, the viability was 88.44% and 54.13%, respectively. MACE ZnO-NPs have anti-cancer effects on Saos2 cells, as demonstrated by the correlation between the results of the MTT assay and the trypan blue exclusion experiment.

Morphological analysis

Another important consideration is the morphological examination of the treated cells to assess the antiproliferation impact of corm ZnO-NPs and Chemically synthesised ZnONPs

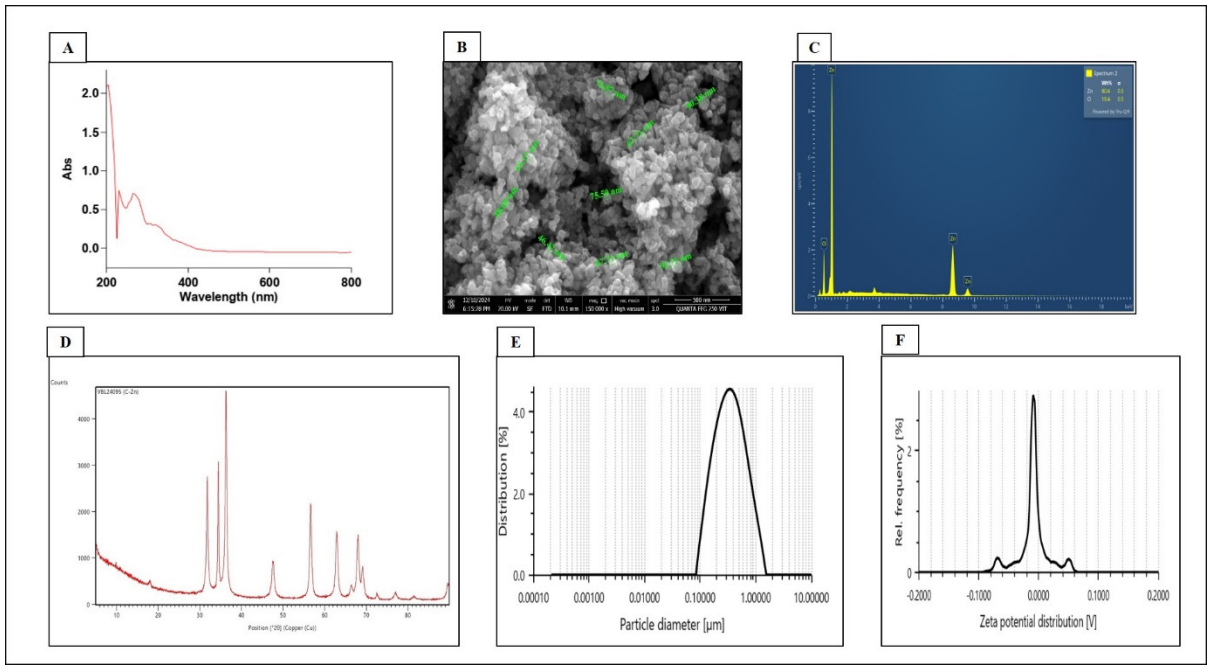

Figure 1: Characterization study of MACE-ZnONPs. A) UV-Spectrometer; B) SEM; C) EDAX; D) XRD; E) Particle size analyzer and F) Zeta potential.

(200, 250, and 300 µg/mL) on Saos2 cells. Compared to the control cells, the treated cells showed more detachment. Additionally, as seen in (Figure 3D), there are noticeable morphological alterations, including cell blebbing, disoriented cells, and shrinkage and rupture.

ROS analysis by DCFH-DA

The DCFH-DA staining method is used to evaluate ROS. Following treatment with the fluorescent dye DCFH-DA, the cells were seen under a microscope. ROS deposition takes place inside saos2 cells upon the addition of MACE-ZnO NPs. As seen in Figure 3E, the fluorescence intensity increased dose-wise as observed in Figure 3D. There is a strong correlation between the levels of ROS and the intensity of fluorescence.

DAPI staining

The nuclear abnormalities of Saos2 cells were investigated using DAPI staining at 200, 250, and 300 µg/mL concentrations. The arrows in Figure 3F indicates apoptotic cells. ZnO-NPs had antiproliferative effect by increasing the number of blue fluorescence cells in a dose-response manner. Condensed nuclei and chromatin disruption were seen in the treated cells. Untreated cells, on the other hand, displayed their natural structure devoid of any abnormalities.

Scratch assay

We investigated effect of MACE-ZnONPs on cell migration in response to the mechanical scratch wound shown in Figure 4. It shows scratch regions at time periods 0, 24, and 48 hr for different concentration. The representative control at each time point showed scratch was half closed in 48 hr whereas on NPs administered in a concentration-dependent manner effectively inhibited cell migration in Saos2 cell lines. After 48 hr of incubation, ZnONPs significantly decreased cell migration in saos2 cells at 300 µg/mL as compared to control.

Oxidative stress markers of LPO and NO

By examining redox imbalance, the primary actor in the cell signaling pathways, the secondary level confirmation of MACE-ZnONPs' anti-cancer effectiveness was investigated by Lipid peroxidation and nitric oxide was determined. Nitric oxide and lipid peroxidation were calculated for the treated and control groups. Figure 5A demonstrated the markedly increased level of LPO generation, whereas Figure 5B demonstrated the elevated level of NO production. The one-way ANOVA was used to examine the results. A significant difference between the treatment and control groups was found using Dunnett's multiple comparison test. Compared to the control cells, the treated cells showed greater significance ($p<0.0001$).

Antioxidant Assay of GSH

Glutathione is a tripeptide that exists in both reduced and oxidized forms. In Saos2 cells treated with developed MACE-ZnO NPs showed a dose-dependent decrease in GSH levels (Figure 5C). The investigation results revealed that the nanoparticles significantly affected glutathione levels. Treated cells showed a significantly greater effect compared to the control cells.

DISCUSSION

Cancer is a global health concern due to its environmental, genetic, and viral causes, affecting 3.4 million people annually. Osteosarcoma is particularly aggressive and often requires intensive treatment such as surgery, chemotherapy, and radiation therapy. However, there are a number of adverse effects and a relatively low success rate with above treatments.[26,27] Nanoparticle-based strategies are being investigated, nevertheless, in an effort to reduce the adverse effects of traditional therapies. Potential therapy options for cancer are being presented by the "phytonano-oncology" field, which blends oncology, nanotechnology, and medicinal plants. Medicinal plants can produce metal or metal oxide nanoparticles and medicinal compounds.[27,28] Zinc oxide nanoparticles (ZnONPs) are gaining attention in nanomedicine due to their potential in cancer

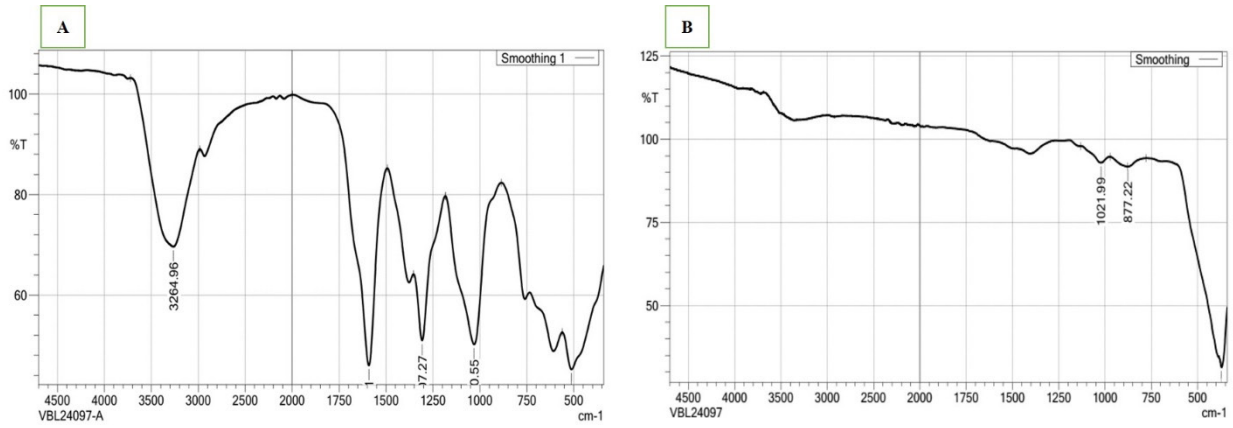

Figure 2: FTIR analysis A) *Musa Acuminata* Corm extract and B) synthesised MACE-ZnONPs.

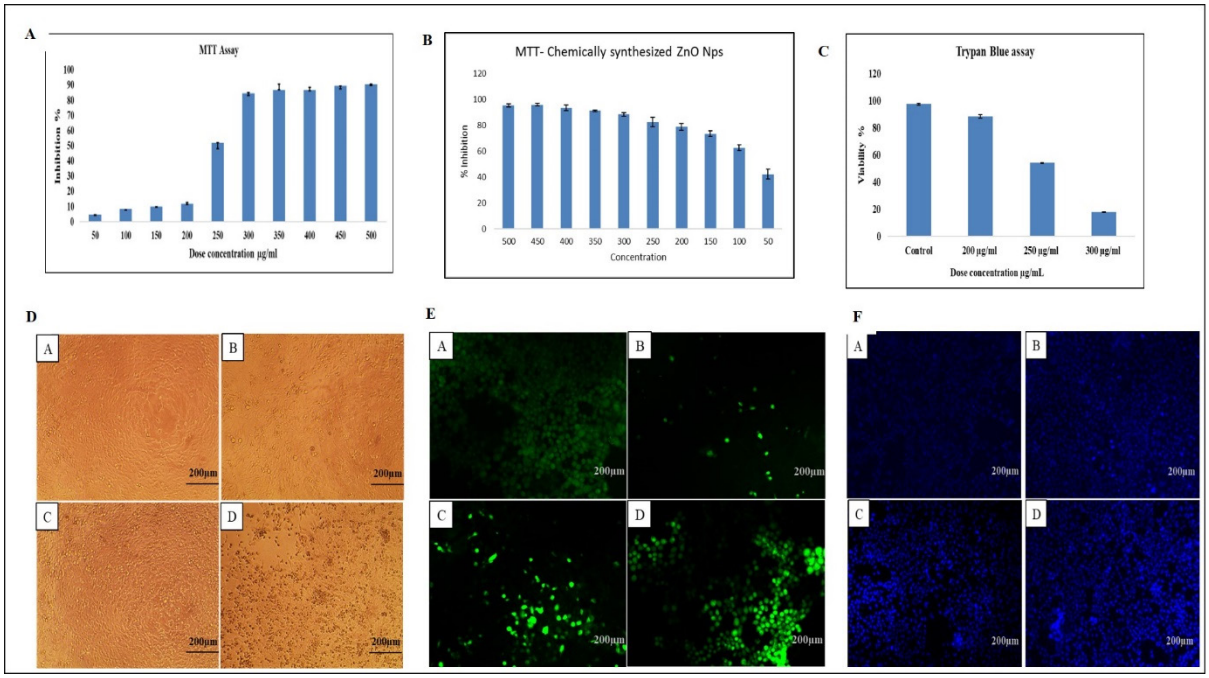

Figure 3: Anti-Cancer activity of MACE-ZnONPs. A) MTT Assay; B)Chemically synthesised ZnONPs; C) Trypan Blue Assay; D) Morphometric analysis; E) ROS by Staining method and F) DAPI Staining.

therapy, as they have been found to induce cytotoxic effects in various cancer cell lines, including breast and ovarian cancer.

Musa acuminata is a very nutrient-dense vegetable that has been shown to have anti-cancer and therapeutic benefits.[29] Organic compounds such as cycloeucalenol acetate, 4-epicyclomusalenone, and Chlorogenic Acid (CA) are found in banana corm, an agricultural waste from tropical banana farms. These substances limit microbiological growth and platelet aggregation, among other biological actions. The culinary and pharmaceutical sectors can benefit greatly from the utilization of banana corms as a source of multipurpose bioactive chemicals.[30] CA is the major compound in corm extract because it has good anticancer property and it is a phenolic category. It encourages the production of the topoisomerase I and II-DNA complex, which is essential for apoptosis, as well as intracellular DNA damage.[31] ZnO NPs have strong anti-cancer properties because of their exceptional capacity to selectively target developing cells. Combining all of these possibilities, the current work examined the anticancer effects of MACE-synthesised zinc oxide nanoparticles on Saos2 cancer cell lines.

Green synthesised ZnO NPs were produced and confirmed using various kinds of characterization techniques. The optical property was characterized and the production of ZnO NPs was confirmed using the UV-vis spectroscopy technique.[32] The reduction of metal oxide and the formation of ZnO NPs from zinc acetate were suggested by the peak absorption seen at 265 nm. The UV spectra of the ZnO NPs are displayed in Figure 1, and the distinctive peak at 265 nm in the UV region proved that the produced NPs are pure ZnO with wurtzite hexagonal phase. The UV analysis found in this investigation is also consistent with previous findings.[33] FT-IR investigation revealed absorption peaks attributed to O-H stretching vibrations (3264 cm^{-1}), indicating the presence of adsorbed water or hydroxyl groups. C-H stretching and bending vibrations cause peaks around 1307 cm^{-1}, which may indicate the presence of surface-adsorbed hydrocarbons or organic residues. The major component was confirmed to be ZnO by the peaks at 512.07 cm^{-1}, which are typical of Zn-O stretching vibrations.[34] The presence of secondary metabolites in the MACE extract is primarily responsible for the spherical and hexagonal-like shapes as well as the unequal aggregation of ZnO-NPs shown in SEM examination.[35] The purity of ZnO-NPs was shown by the EDAX pattern, which showed peaks of zinc in the main form coupled with oxygen.[36,37] ZnO-NPs had a zeta potential of -0.0122 V, which indicates superior coagulation ability and increased stability. The ZnO NPs are said to have high stability since the negative sign of the zeta potential value guarantees the repulsion between the particles.[38] Zeta potential and particle size distribution results showed a strong correlation.[39] The XRD peaks that were found match the JCPDS card number 75-0576, which shows that ZnO has a hexagonal wurtzite phase. The ZnO-NPs' crystalline nature and phase purity are further confirmed by the detected peaks at certain 2θ angles, which correlate to specific lattice planes.[40,41]

MACE-ZnO NPs-treated cells decreased the survival of the saos2 cell line in a dose-dependent manner, with an acceptable value (LC_{50}) 49.11% at 250 µg/ml of synthesized NPs, which is consistent with the previous data published by Ruangtong in 2020.[42] To further verify the MTT data, a trypan blue dye cell viability experiment was conducted. The dose-response anti-cancer activity of ZnO-NPs was demonstrated by the

decreasing number of viable cells in the treated groups as dosage increased. Chemically synthesized nanoparticles are more toxic and shows lower IC_{50} due to smaller size, lack of protective coating, higher ROS generation whereas plant based ZnONps possesses high IC_{50} with less toxicity due to natural capping agent which reduces oxidative stress and enhance the biocompatibility. Phase contrast microscopic studies, Saos2 cells treated with ZnO-NPs showed detached cells with disoriented architecture as well as rounding and shrinking of the cells. The cytotoxicity of ZnO-NPs was confirmed by the treated cells with damaged cell membranes when compared to the control morphology.[43] Cancer has a unique ability to spread to other organs by cell-to-cell movement, or metastasis, in addition to unchecked divisions. By using the scratch assay on saos2 cell lines, we were able to demonstrate the concentration-dependent and efficient cell migration-inhibiting capacity of biologically synthesized ZnONPs (Figure 4). After 48 hr of incubation, nanoparticles significantly decreased cell migration in saos2 cells at 300 µg/mL in comparison to the control. NPs capacity to disrupt the cytoskeleton of the cell may be the cause of their suppression of saos2 migration. Cytoskeleton rearrangement is necessary for cell division and migration, and disruption of one or both processes has a significant impact on these activities. Our findings are consistent with those of previous research.[44,45]

To get rid of cells without harming other cells, apoptosis a planned sequence of events that coordinates cell death is essential. It is crucial to maintain the balance between cell division and cell death, which supports healthy tissue homeostasis. Numerous NPs have been shown to cause cancer cells to undergo apoptosis, which suggests that they may be used as anticancer treatments.[46] In DAPI staining, the dye binds to cells with blue fluorescence, and the intensity increased with higher doses, indicating a condensed nucleus with apoptotic signs like cell shrinkage, nuclear condensation, and detachment from the surface.[47] ROS is essential for pathogenic activities, such as cell division, oxidative defense, and the destruction of invading pathogens. ROS was confirmed by DCFH-DA's assessment of fluorescence intensity. Saos2 cells, which represent intact cells and early apoptotic cells,

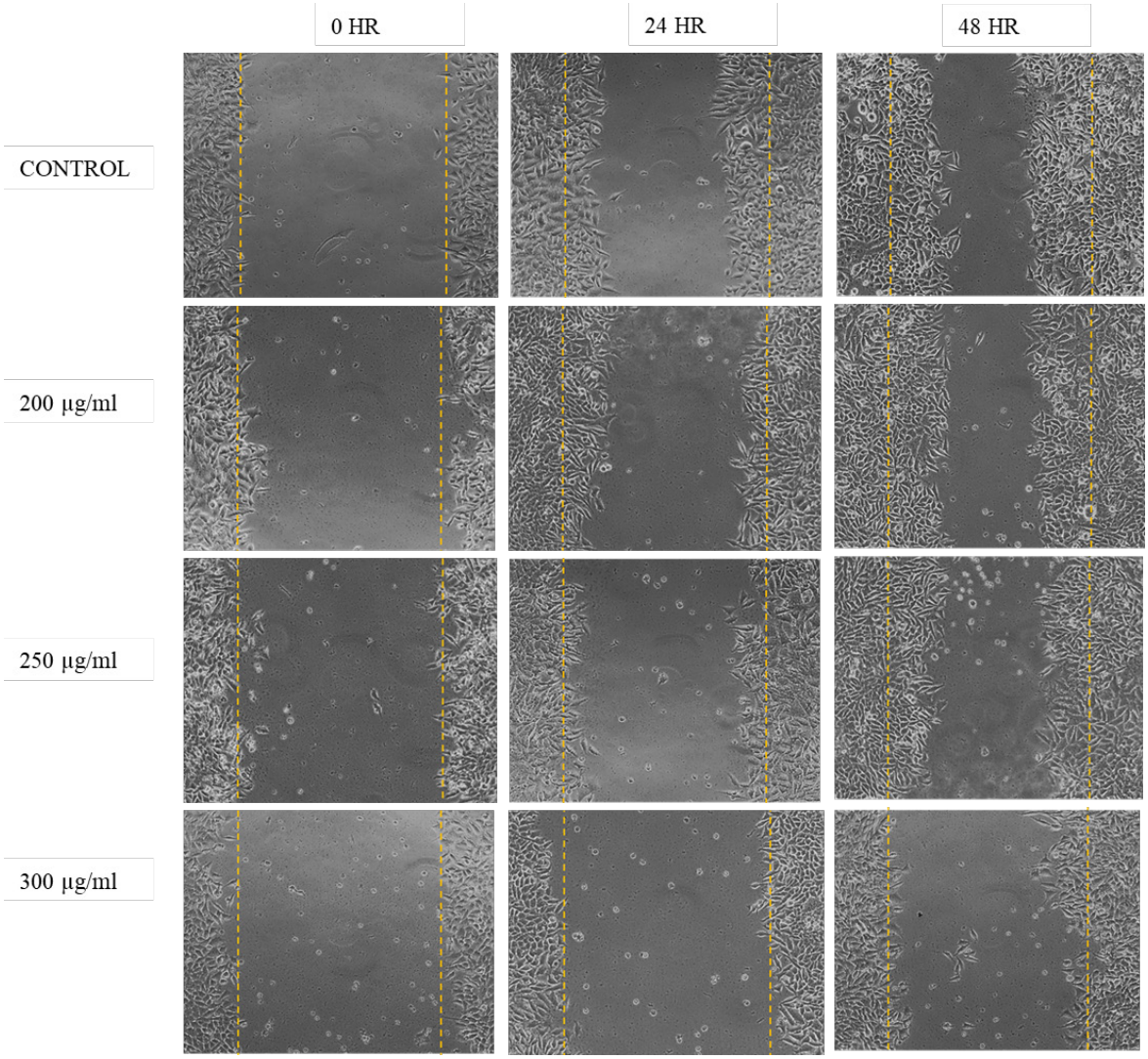

Figure 4: Wound healing Assay (scratch assay).

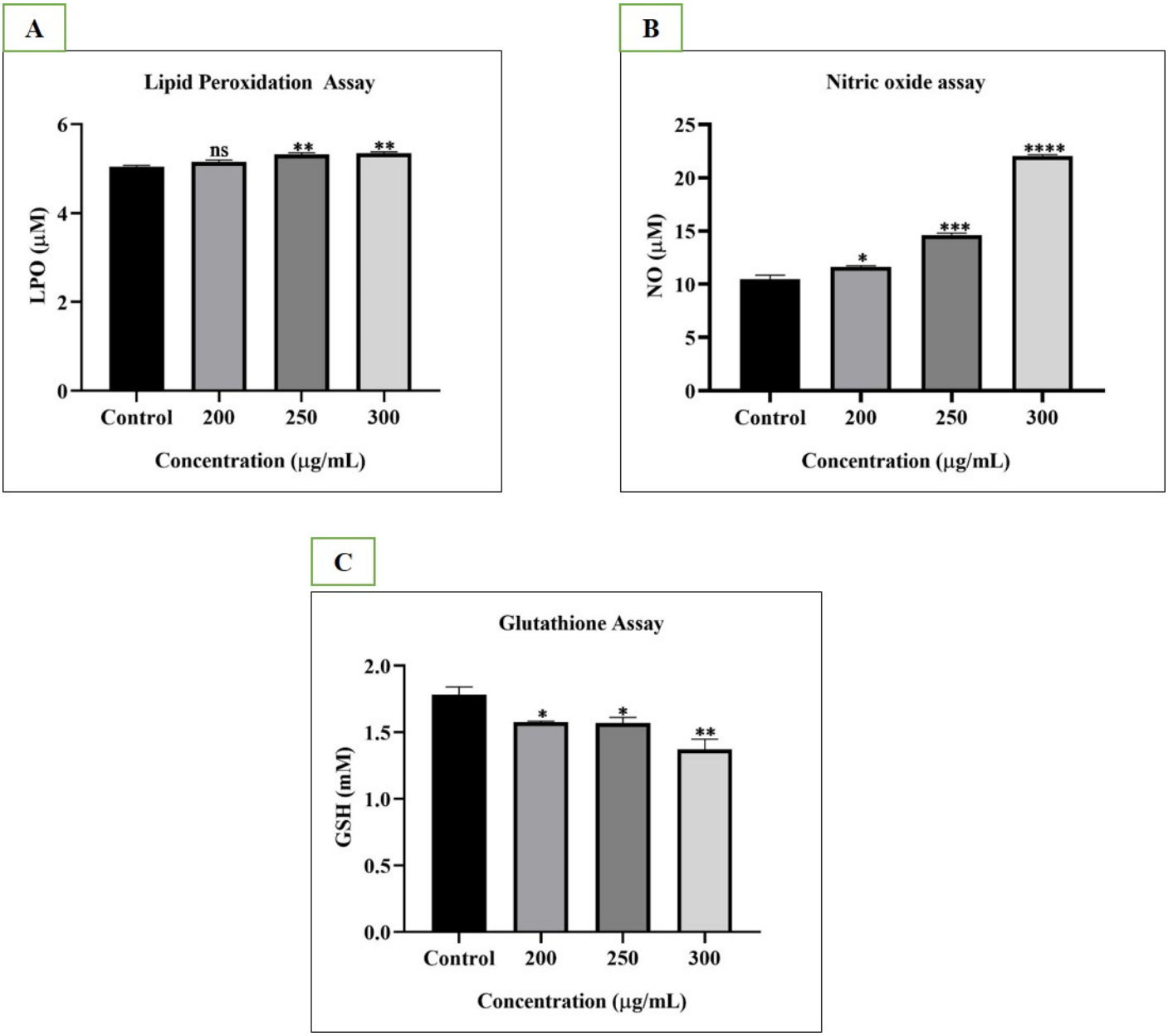

Figure 5: Oxidative stress markers. A) LPO Assay B) NO Assay and C) GSH Assay.

experienced concentration-dependent apoptosis in response to MACE-ZnONPs at lower nanoparticle concentrations. We saw very few late apoptotic cells. At the medium dosage, a greater proportion of cells underwent both early and late apoptosis. On the other hand, a higher concentration of NPs led to more apoptotic cells. One of the negative effects of unregulated ROS is lipid peroxidation. The general structure of the cell may be impacted by lipid membrane peroxidation, which also makes the lipid membrane less fluid, ultimately leading to the loss of cellular integrity.[48,49] Significant lipid peroxidation can trigger the death process and in our study dose-dependent increase was seen on NP exposure (Figure 5A). Nitric oxide has the potential to negatively affect apoptosis.[50] As a result, the amount of nitric oxide produced by Saos2 cells in response to NPs coated with corm extract was measured. NO levels, along with other key markers of oxidative stress, were elevated in the treated groups. The findings of the study suggest that MACE ZnO NPs induce oxidative stress in a manner similar to what was described in.[51]

Glutathione is a naturally occurring antioxidant that shields cells from oxidative damage.[52] Following a 24-hr exposure to MACE-coated ZnO NPs, cancer cells showed reduced glutathione levels. This weakens the cellular antioxidant defense mechanism, which damages and ultimately induces apoptosis.[53] Since we synthesized the ZnO-NPs through a phytogenic process using *Musa acuminata* corm extract, which also contains phytocompounds with notable anti-cancer properties, the ability of ZnO-NPs to inhibit Saos2 cell growth is further amplified.

Overall, biogenically produced ZnO-NPs exhibit a potent anti-cancer effect on Saos2 cells.

CONCLUSION

In conclusion, we successfully green synthesized ZnO NPs and demonstrated their anticancer activity against Saos2 cells. The characterization of the ZnO NPs was performed using FT-IR, DLS, SEM, XRD, and UV analysis. ROS staining confirmed the occurrence of apoptosis, supported with cytotoxicity and DAPI staining in Saos2 cells in dose-dependent manner. Further assessment through antioxidant and oxidative stress markers revealed reduction in GSH activity, along with an increase in LPO and NO levels. This study suggests that ZnO NPs with MACE could be promising for targeted delivery applications, preventing cancer cell growth by inducing apoptosis.

ACKNOWLEDGEMENT

I would like to express my sincere thanks to Research, Development, and Innovation Authority (RDIA) - Kingdom of Saudi Arabia.

ABBREVIATIONS

MACE: *Musa acuminata* Corm extract; **SEM:** Scanning electron microscope; **FTIR:** Fourier electron microscope; **XRD:** X-ray Diffraction; **CA:** Chlorogenic acid; **LPO:** Lipid peroxidation; **NO:** Nitric oxide; **GSH:** Glutathione; **DCFH-DA:** Dichloro-dihydro-fluorescein diacetate.

CONFLICT OF INTEREST

The authors declare that there is no conflict of interest.

FUNDING

This article is derived from a research grant funded by the Research, Development, and Innovation Authority (RDIA) - Kingdom of Saudi Arabia - with grant number (12894-JAZZAN-2023-JZU-R-2-1-SE).

SUMMARY

This study explores the anticancer potential of green-synthesized zinc oxide nanoparticles (ZnO NPs) coated with *Musa acuminata* corm extract (MACE) against Saos2 osteosarcoma cells. Characterized using UV-Vis, SEM, FTIR, DLS, and XRD, the NPs displayed a hexagonal structure, high purity (50.37% Zn, 49.63% O), and stability (zeta potential -0.0122 V). Cytotoxicity assays (MTT, trypan blue) revealed significant cell inhibition (IC50 300 µg/mL, 49.36% inhibition), with morphological distortions and reduced viability (18.17% at 300 µg/mL). DAPI and ROS staining confirmed dose-dependent apoptosis, while increased LPO and NO and decreased GSH levels indicated oxidative stress. Scratch assays showed inhibited cell migration, suggesting MACE-ZnO NPs as a biocompatible, targeted therapy for osteosarcoma.

REFERENCES

1. Miser JS, Pritchard DJ, Rock MG, *et al.* Osteosarcoma in adolescents and young adults: new developments and controversies. Springer Science+Business Media; 2012.
2. Bodmer N, Hecker-Nolting S, Friedel G, Blattmann C, Kager L, Kessler T, *et al.* Primary osteosarcoma of the ribs: a report from the cooperative osteosarcoma study group. Cancer. 2023; 129(12): 1895-903. doi: 10.1002/cncr.34744, PMID 36928868.
3. Livshits Z, Rao RB, Smith SW. An approach to chemotherapy-associated toxicity. Emerg Med Clin North Am. 2014; 32(1): 167-203. doi: 10.1016/j.emc.2013.09.002, PMID 24275174.
4. Kumari S, Goyal A, Sönmez Gürer E, Algın Yapar E, Garg M, Sood M *et al.* Bioactive loaded novel nano-formulations for targeted drug delivery and their therapeutic potential. Pharmaceutics. 2022; 14(5): 1091. doi: 10.3390/pharmaceutics14051091, PMID 35631677.
5. Saw PE, Lee S, Jon S. Naturally occurring bioactive compound-derived nanoparticles for biomedical applications. Adv Ther. 2019; 2(5): 1800146. doi: 10.1002/adtp.201800146.
6. Czylkowska A, Rogalewicz B, Szczesio M, Raducka A, Gobis K, Szymański P, *et al.* Antitumor activity against A549 cancer cells of three novel complexes supported by coating with silver nanoparticles. Int J Mol Sci. 2022; 23(6): 2980. doi: 10.3390/ijms23062980, PMID 35328401.
7. Alkarkhi M, AF, bin Ramli S. Shin Yong Y, Mat Easa A. Asian Journal of Food and. Agro-Industry Physicochemical properties of banana peel flour as influenced by variety and stage of ripeness: multivariate statistical analysis. As J Food Ag-Ind [Internet]. 2010; 3(3): 349-62.
8. Mathew NS, Negi PS. Traditional uses, phytochemistry and pharmacology of wild banana (*Musa acuminata* Colla): a review. J Ethnopharmacol. 2017; 196: 124-40. doi: 10.1016/j.jep.2016.12.009, PMID 27988402.
9. Oresanya IO, Sonibare MA, Gueye B, Balogun FO, Adebayo S, Ashafa AOT, *et al.* Isolation of flavonoids from *Musa acuminata* Colla (Simili radjah, ABB) and the *in vitro* inhibitory effects of its leaf and fruit fractions on free radicals, acetylcholinesterase,15-lipoxygenase, and carbohydrate hydrolyzing enzymes. J Food Biochem. 2020; 44(3): e13137. doi: 10.1111/jfbc.13137, PMID 31899556.
10. Ramu V, Kumar Krishnamurthy G, Kumar GK, Kumar R SS. Antibacterial activity of ethanol extract of *Musa paradisiaca* cv. Puttabale and *Musa acuminate* cv. grand naine DICHROSTACHYS CINEREA View project Bioprospecting of Medicinal Plants of Western Ghats, Karnataka View project ANTIBACTERIAL ACTIVITY OF ETHANOL EXTRACT OF *MUSA PARADISIACA* CV. PUTTABALE AND *MUSA ACUMINATE* CV.GRAND NAINE [Internet]. Article in Asian Journal of Pharmaceutical and Clinical Research. 2013.
11. Hamidian, K. *et al.* Doped and un-doped cerium oxide nanoparticles: Biosynthesis, characterization, and cytotoxic study. Ceramics Int. 47(10, Part A), 13895-13902 (2021).
12. Haghighat, M. *et al.* Cytotoxicity properties of plant-mediated synthesized K-doped ZnO nanostructures. Bioprocess Biosyst. Eng. 45(1), 1-8 (2022).
13. Liang X, Zhang D, Liu W, Yan Y, Zhou F, Wu W, Yan Z. Reactive oxygen species trigger NF-κB-mediated NLRP3 inflammasome activation induced by zinc oxide nanoparticles in A549 cells. Toxicology and Industrial Health. 2017; 33(10): 737-45.
14. Akhtar MJ, Ahamed M, Kumar S, Khan MM, Ahmad J, Alrokayan SA. Zinc oxide nanoparticles selectively induce apoptosis in human cancer cells through reactive oxygen species. International journal of nanomedicine. 2012: 845-57.
15. Anjum S, Hashim M, Malik SA, Khan M, Lorenzo JM, Abbasi BH, *et al.* Recent advances in zinc oxide nanoparticles (Zno nps) for cancer diagnosis, target drug delivery, and treatment. Cancers (Basel). 2021; 13(18).
16. Yashni G, Al-Gheethi AA, Mohamed RM, Hashim MA. Green synthesis of ZnO NPs by *Coriandrum sativum* leaf extract: structural and optical properties. Desalination and Water Treatment. 2019; 167: 245-57.
17. Mosmann T. Rapid Colorimetric Assay for Cellular Growth and Survival: Application to Proliferation and Cytotoxicity Assays. Vol. 65, Journal of Immuno logical Methods. 1983.
18. Yuan YG, Zhang S, Hwang JY, Kong IK. Silver nanoparticles potentiates cytotoxicity and apoptotic potential of camptothecin in human cervical cancer cells. Oxid Med Cell Longev. 2018; 2018.
19. Chen X, Zhao X, Gao Y, Yin J, Bai M, Wang F. Green synthesis of gold nanoparticles using carrageenan oligosaccharide and their *in vitro* antitumor activity. Mar Drugs. 2018; 16(8).
20. Wang X, Decker CC, Zechner L, Krstin S, Wink M. *In vitro* wound healing of tumor cells: inhibition of cell migration by selected cytotoxic alkaloids. BMC Pharmacology and Toxicology. 2019; 20: 1-2.
21. Raja Singh P, Arunkumar R, Sivakamasundari V, Sharmila G, Elumalai P, Suganthapriya E, *et al.* Anti-proliferative and apoptosis inducing effect of nimbolide by altering molecules involved in apoptosis and IGF signalling via PI3K/Akt in prostate cancer (PC-3) cell line. Cell Biochem Funct. 2014; 32(3): 217-28.

22. Silveira, L. R., Pereira-Da-Silva, L., Juel, C., and Hellsten, Y. Formation of hydrogen peroxide and nitric oxide in rat skeletal muscle cells during contractions. Free Radic. Biol.Med. 2003; 35(5): 455-464. DOI: 10.1016/s0891-5849(03)00271-5
23. Wahyuni FS, Ali DAI, Lajis NH, Dachriyanus. Anti-inflammatory activity of isolated compounds from the Stem Bark of Garcinia cowa Roxb. Pharmacognosy Journal. 2017; 9(1): 55-7.
24. Ohkawa H, Ohishi N, Yagi K. Assay for Lipid Peroxides in Animal Tissues by Thiobarbituric Acid Reaction. Vol. 95, ANALYTICAL BIOCHEMISTRY. 1979.
25. Goh H, Kadir HA. *In vitro* cytotoxic potential of Swietenia macrophylla King seeds against human carcinoma cell lines. Journal of Medicinal Plants Research [Internet]. 2011; 5(8): 1395-404. Available from: http://www.academicjournals.org/JMPR
26. Misaghi A, Goldin A, Awad M, Kulidjian AA. Osteosarcoma: A comprehensive review. Vol. 4, SICOT-J. EDP Sciences; 2018.
27. Hameed S, Iqbal J, Ali M, Khalil AT, Abbasi BA, Numan M, *et al.* Green synthesis of zinc nanoparticles through plant extracts: Establishing a novel era in cancer theranostics. Vol. 6, Materials Research Express. Institute of Physics Publishing; 2019.
28. Akhtar MJ, Ahamed M, Kumar S, Khan MAM, Ahmad J, Alrokayan SA. Zinc oxide nanoparticles selectively induce apoptosis in human cancer cells through reactive oxygen species. Int J Nanomedicine. 2012; 7: 845.
29. Vijay N, Shashikant D, Mohini P. Assessment of antidiabetic potential of *Musa acuminata* peel extract and its fractions in experimental animals and characterization of its bioactive compounds by HPTLC. Arch Physiol Biochem. 2022; 128(2): 360-72. doi: 10.1080/13813455.2019.1683585, PMID 31687854
30. Fajrih N, Wiryawan KG, SUMIATI S, Syahpura SK, Winarsih W. Identification of bioactive compounds of banana corm (*Musa paradisiaca*) using GC-MS and its inhibitory effect against pathogenic bacteria. Biodiversitas Journal of Biological Diversity. 2022; 23(1).
31. Gupta A, Atanasov AG, Li Y, Kumar N, Bishayee A. Chlorogenic acid for cancer prevention and therapy: Current status on efficacy and mechanisms of action. Pharmacological Research. 2022; 186: 106505.
32. Senthilkumar N, Nandhakumar E, Priya P, Soni D, Vimalan M, Potheher IV. Synthesis of ZnO NPs using leaf extract of *Tectona grandis* (L.) and their anti-bacterial, anti-arthritic, anti-oxidant and *in vitro* cytotoxicity activities. New Journal of Chemistry. 2017; 41(18): 10347-56.
33. Yang X, Cao X, Chen C, Liao L, Yuan S, Huang S. Green Synthesis of Zinc Oxide Nanoparticles Using Aqueous Extracts of Hibiscus cannabinus L.: Wastewater Purification and Antibacterial Activity. Separations. 2023; 10(9): 466.
34. Reddy MS, Singh KP, Kumar N, Kumar R, Singh MV, Gupta S. Multifaceted applications of chitosan-L-ornithine modified ZnO NPs: Antibacterial, antioxidant, and anticancer potentials. J Drug Deliv Sci Technol. 2024; 91.
35. Gurgur E, Oluyamo SS, Adetuyi AO, Omotunde OI, Okoronkwo AE. Green synthesis of zinc oxide nanoparticles and zinc oxide-silver, zinc oxide-copper nanocomposites using *Bridelia ferruginea* as biotemplate. SN Appl Sci. 2020; 2(5).
36. Kallappa D, Venkatarangaiah VT. Synthesis of CeO2 doped ZnO NPs and their application in Zn-composite coating on mild steel. Arabian Journal of Chemistry. 2020; 13(1): 2309-17.
37. Nagarajan S, Kuppusamy KA. Extracellular synthesis of zinc oxide nanoparticle using seaweeds of gulf of Mannar, India [Internet]. 2013.
38. Umamaheswari A, Prabu SL, John SA, Puratchikody A. Green synthesis of zinc oxide nanoparticles using leaf extracts of *Raphanus sativus* var. Longipinnatus and evaluation of their anticancer property in A549 cell lines. Biotechnology Reports. 2021; 29: e00595.
39. Barzinjy AA, Azeez HH. Green synthesis and characterization of zinc oxide nanoparticles using *Eucalyptus globulus* Labill. leaf extract and zinc nitrate hexahydrate salt. SN Appl Sci. 2020; 2(5).
40. Sun Y, Guo H, Zhang W, Zhou T, Qiu Y, Xu K, *et al.* Synthesis and characterization of twinned flower-like ZnO structures grown by hydrothermal methods. Ceram Int. 2016; 42(8): 9648-52.
41. Mustapha S, Ndamitso MM, Abdulkareem AS, Tijani JO, Shuaib DT, Mohammed AK, *et al.* Comparative study of crystallite size using Williamson-Hall and Debye-Scherrer plots for ZnO NPs. Advances in Natural Sciences: Nanoscience and Nanotechnology. 2019; 10(4).
42. Ruangtong J, Jiraroj T, T-Thienprasert NP. Green synthesized ZnO nanosheets from banana peel extract possess anti-bacterial activity and anti-cancer activity. Materials Today Communications. 2020; 24: 101224.
43. Hirad AH, Alarfaj AA, Ravindran B, Narasimhamoorthi SP. Betanin inspired zinc oxide nanoparticles: The potential antioxidant and anticancer activity against human lung cancer cell line (A549). Biochemical and Biophysical Research Communications. 2025; 742: 151019.
44. Buranasukhon W, Athikomkulchai S, Tadtong S, Chittasupho C. Wound healing activity of *Pluchea indica* leaf extract in oral mucosal cell line and oral spray formulation containing nanoparticles of the extract. Pharmaceutical Biology. 2017; 55(1): 1767-74.
45. Khan, M.S.; Tabrez, S.; Al-Okail, M.S.; Shaik, G.M.; Bhat, S.A.; Rehman, M.T.; Husain, F.M.; AlAjmi, M.F. Non-enzymatic glycation of protein induces cancer cell proliferation and its inhibition by quercetin: Spectroscopic, cytotoxicity and molecular docking studies. J. Biomol. Struct. Dyn. 2021, 9, 777-786.
46. Hussain A, *et al.* Biogenesis of ZnO NPs using *Pandanus odorifer* leaf extract: Anticancer and antimicrobial activities. RSC Adv. 2019; 9: 15357-15369. doi: 10.1039/C9RA01659G.
47. Saraste A, Pulkki K. Morphologic and biochemical hallmarks of apoptosis [Internet]. Vol. 45, Cardiovascular Research. 2000.
48. Dix TA, Aikens J. Mechanisms and biological relevance of lipid peroxidation initiation. Chem Res Toxicol. 1993; 6(1): 2-18.
49. Zughaibi TA, Mirza AA, Suhail M, Jabir NR, Zaidi SK, Wasi S, *et al.* Evaluation of Anticancer Potential of Biogenic Copper Oxide Nanoparticles (CuO NPs) against Breast Cancer. J Nanomater. 2022; 2022
50. Hwang JH, Park SJ, Ko WG, Kang SM, Lee D Bin, Bang J, *et al.* Cordycepin induces human lung cancer cell apoptosis by inhibiting nitric oxide mediated ERK/Slug signaling pathway. Am J Cancer Res. 2017; 7(3): 417
51. Saim, A. K.; Kumah, F. N.; Oppong, M. N. Extracellular and intracellular synthesis of gold and silver nanoparticles by living plants: A review. Nanotechnol. Environ. Eng. 2021, 6, 1, DOI: 10.1007/s41204-020-00095-9
52. Forman HJ, Zhang H, Rinna A. Glutathione: overview o0066 its protective roles, measurement, and biosynthesis. Mol Aspects Med. 2009; 30(1-2): 1-12.
53. Alyami NM, Almeer R, Alyami HM. Role of green synthesized platinum nanoparticles in cytotoxicity, oxidative stress, and apoptosis of human colon cancer cells (HCT-116). Heliyon. 2022; 8(12).

Cite this article: Rym H. Green Synthesized Zinc Oxide Nanoparticles Using *Musa acuminata* Corm Extract and Its Anti-Cancer Activity. Indian J of Pharmaceutical Education and Research. 2026;60(2):642-51.